Electronic Supplementary Material (ESI) for Physical Chemistry Chemical Physics.

Searching for correlations between geometric and spectroscopic parameters of intramolecular hydrogen bonds in porphyrin-like macrocycles

Sylwester Gawinkowski, Om Prakash

Table of Contents:

I. Tables of experimental data obtained from the literature

All experimental data analysed in this work were obtained from the literature. All compound names listed in the tables correspond to the original names used in the respective references.

Table S1. Experimental values of N…N distances, NH bond lengths, IR/Raman frequencies, and ^{1}H chemical shifts of porphycenes.

Table S2. Experimental values of N…N distances, NH bond lengths, IR/Raman frequencies, and ^{1}H chemical shifts of porphyrins.

Table S3. Experimental values of N…N distances, NH bond lengths, IR/Raman frequencies, and ^{1}H chemical shifts of dibenzotetraaza[14]annulenes.

Table S4. Experimental values of N…N distances, NH bond lengths, IR/Raman frequencies, and ^{1}H chemical shifts of different macrocycles with double intramolecular hydrogen bonds.

Table S1							
No.	**Name**	**N1N2 distance (ppm)**	**N2N3 distance (ppm)**	**ν(NH) IR (cm^{-1})**	**ν(NH) Raman (cm^{-1})**	**NMR**	**References**
1.	porphycene	262.5	282.8	2500-2800		3.15	1-3
2.	9,10,19,20-tetramethylporphycene	253.2	291.2			6.67	4, 5
3.	9,10,19,20-tetra-n-propylporphycene	252.8	289.8			6.82	6
4.	9,10,19,20-tetrphenylporphycene	254.7	287.4			5.98	7
5.	9,10,19,20-tetraoctylporphycene	253	289.8			6.85	5
6.	CF3Pc	255.2	289.4			5.68	7
7.	FPc	256.2	286.6			5.66	7
8.	CH_3Pc	256.8	287.3			5.94	7
9.	OAPo-T	258.4	286.7			5.67	8
10.	3b	251.9	296			6.81	9
11.	1a	260.2	289.8			5.5	9
12.	1c	269.4	280.5			0.8	9
13.	2,7,12,17-tetraethyl-3,6,13,16-tetramethylporphycene	279.1	273.7			0.86	10
14.	2,3,6,7,12,13,16,17-octaethylporphycene	279.9	273.2			0.65	10
15.	Cy6Pc	255.5	289.7			6.7	11
16.	Cy5Pc	260.5	286.9			4.96	11
17.	mMBPc	257.8	289			7.85	12
18.	mMBPc*	258.9	289			7.47	12
19.	mDBPc	253.4	294			8.83	12
20.	2,7,12,17-tetrapropylporphycene	261.5	283.1			3.04	13
21.	2,7,12,17-tetra-tert-butylporphycene					3.58	4, 14
22.	2,7,12,17-tetraphenylporphycene	263.5	284.3			3.5	15, 16
23.	2,7,12,17-tetra(p-trifluoromethylphenyl)-porphycene					3.92	16
24.	2,7,12,17-tetra(p-methoxyphenyl)-porphycene	260.8	286.3			3.77	16
25.	2,7,12,17-tetraisopropyldinaphthoporphycene	249.1	294.7			9.27	17
26.	2,7,12,17-tetra-(*tert*-butyl)-3,6-13,16-dibenzo[*cde*;*mno*]porphycene	251				10.57	18
27.	2,7,12,17-tetra-*n*-propylporphycene	262				3.15	18
28.	3,6,13,16-tetramethoxyporphycene	271.1	277.2			0.82	19
29.	2,3,6,7,12,13,16,17-octamethoxyporphycene	275.8	274.1			0.36	20
30.	*β*-tetrakis (trifluoromethyl)porphycene	268.3	276.6			2.33	21
31.	12,17-tetraethyl-3,6,13,16-tetrakis(trifluoromethyl)porphycene	263.1	282.7			2.65	22
32.	3-bromo-2,7,12,17-tetrapropylporphycene	266.6	281.3			1.69	22
33.	3,13-dibromo-2,7,12,17-tetrapropylporphycene	272.3	274.4			1.51	22
34.	3,6,13-tribromo-2,7,12,17-tetrapropylporphycene	271.1	278.7			1.15	22

35.	3,6,13,16-tetrabromo-2,7,12,17-tetra-propylporphycene	273.4	281.3			3.6	23
36.	2,3,7,12,13,17-hexaethylporphycene	280.5	271			0.39	24
37.	2,3,6,12,13,16-hexaethylporphycene	267	279.7			2.08	24
38.	BHPcH2	267.9	279.8			2.77	25, 26
39.	9,10-diacetoxy-2,7,12,17-tetrapropylporphycene	259.6	284.8			4.32	27
40.	9,10-diacetoxy-2,7,12,17-tetrapropylporphycene*	261.1	285.7			3.67	27
41.	3,3'-(Buta-1,3-diyne-1,4-diyl)-bis(2,7,12,17-tetrahexylporphycene)	264.4				2.75	28
42.	3,3'-(Buta-1,3-diyne-1,4-diyl)-bis(2,7,12,17-tetrahexylporphycene)*	263.3				3.04	28
43.	9,10,19,20-tetrakis(but-1-en-4-yl)porphycene	254.2	289.9			6.82	29
44.	2,3,6,7,12,13,16,17-octa(methylthio)porphycene	269.4	276.2			2.98	30
45.	2,7,12,17-tetrachloro-3,6,13,16-tetramethoxyporphycene	271.5	278			0.98	31
46.	3,6,13,16-tetrachloro-2,7,12,17-tetramethoxyporphycene*	276.1	272.7			0.16	31
47.	Compound-18	255.7	286.8			5.87	32
48.	Compound-8	254.4	287.5			5.91	32
49.	Compound-9	256.2	285.9			5.84	32
50.	Compund-10	255.3	287.2			5.84	32
51.	Compound-12	257	287.2			5.73	32
52.	2,7,12,17-tetra(5-hexyl-thien-2-yl)porphycene	264.2	283.8			2.59	33

* - two different molecular structures in the crystal or two different NN distances in one structure

Table S2

No.	Name	N1N2 distance (ppm)	N2N3 distance (ppm)	ν(NH) IR (cm^{-1})	ν(NH) Raman (cm^{-1})	NMR	References
1.	porphyrin	289.1	290.8	3330	3366	-3.76	34-39
2.	5-(2-pyrrolyl)porphyrin	282.5	299.1			-3.02	38
3.	2,3,7,8,12,13,17,18-octaethyl-5,10-diphenylporphyrin	288.6	292.7	3325		-2.68	39, 40
4.	2,3,7,8,12,13,17,18-octaethyl-5,15-diphenylporphyrin			3101			39, 40
5.	2,3,7,8,12,13,17,18-octaethyl-5,10,15-triphenylporphyrin	284.2	296.3			-2.11	39
6.	*meso*-tetraphenyl porphyrin	289	289	3311		-3.6	42, 43
7.	2,8,12,18-tetrabutyl-3,7,13,17-	269.2	320.7			-2.42	44
8.	tetramethyl-5-(4-pyridyl)porphyrin	272.7	315.9			-2.51	44
9.	2,3,5,7,8,12,13,15,17,18-decaalkylporphvrins	263	329			-1.78	45
10.	2,8,12,18-tetra-n-butyl-5,15-bis(4-hexyloxyphenyl)-3,7,13,17-tetramethylporphyrin	274.6	315.5				46
11.	2,8,12,18-tetra-n-butyl-5,15-bis(4-octyloxyphenyl)-3,7,13,17-tetramethylporphyrin	271.7	316.1			-2.45	46
12.	5,15-diphenyl-2,8,12,18-tetraethyl-3,7,13,17-tetramethylporphyrin	269.6	317.4				47
13.	5,15-bis(3-hydroxyphenyl)-	274.6	317.1			-2.64	47
14.	5,15-bis(4-cyanophenyl)-2,8,12,18-tetra-n-hexyl-3,7,13,17-tetramethylporphyrin	271.7	317.4			-2.48	47
15.	5,15-bis(3-hydroxyphenyl)-porphyrin, 5,15-diarylporphyrin, 5,15-dialkylporphyrins, 5,15-disubstituted porphyrin	281.6	303.4			-3.2	47-49
16.	5,15-bis(ethyl) porphyrin	277.6	305.5			-2.92	50
17.	5,15-bis(n-butyl) porphyrin	278.7	303.7			-2.91	50
18.	5,15-di-n-butyl-2,3,7,8,12,13,17,18-octaethylporphyrin	264.3	325.8			-1.53	51
19.	1-w	281.8	288.1			-0.61	52
20.	2-w	285.2	291.7			-1.81	52
21.	3-w	287.1	290.1			-2.23	52
22.	4-w	290.1	292.4			-2.55	52
23.	1-s	284.1	288.6			-0.41	52
24.	2-s	284.5	289.4			-1.3	52
25.	3-s	288.6	290.6			-2.14	52
26.	4-s	289.5	292.7			-2.55	52
27.	1-r	271.6	279.1			0.08	52
28.	2-r	270.3	282.3			0.09	52
29.	3-r	285.5	288.9			-0.88	52
30.	4-r	288	289.8			-1.8	52

31.	5,10,15,20-tetraphenyl-2,3,7,8,12,13,17,18-octakis(phenyl-ethynyl)porphyrin	293.4	296.7	3320			53
32.	5,10,15,20-tetrakis(2,6-dibromo-3,4,5-trimethoxyphenyl) porphyrin	289.6	291			-2.38	54
33.	2,3,7,8,12,13,17,18-octaisopropylporphyrin	291	293.2			-3.88	55
34.	5-cyano-2,3,7,8,12,13,17,18-octamethoxyporphyrin	278.1	303.7			-4.17	56
35.	2,3,7,8,12,13,17,18-octamethoxyporphyrin	279	303.7			-4.82	57
36.	2,3,7,8,12,13,17,18-octaethyl-5,10,15,20-tetrakis(2-phenylethynyl)-21H,23H-porphine	286.9	292.4			0.26	58
37.	5,15-(4, 11-diaza-3, 12-dioxotetradecan- I , 14-diyl)-2,8.12,18-tetraethyl-3,7,13,17-tetramethylporphyrin			2850		-1.6	59
38.	ethioporphin	298.5	298.5	3314		-3.74	60
39.	octaethylporphin	291.6	291.6	3310		-3.74	61

Table S3							
No.	**Name**	**N1N2 distance (ppm)**	**N2N3 distance (ppm)**	**ν(NH) IR (cm^{-1})**	**ν(NH) Raman (cm^{-1})**	**NMR**	**References**
1.	dibenzo[14]tetraazaannulene	279.5	267.5	3187	3185	13.96	63, 64
2.	7,16-dihydro-6,8,15,17-tetramethyl-dibenzo(b,i)(1,4,8,11)tetra-azacyclotetradecine	267.6	270	3064	3048	12.59	65, 66
3.	4,11-dihydro-6,13-dimethyl-2,3:9,10-dibenzo-1,4,8,11-tetrazacyclotetradeca-5,7,12,14-tetraene	275.3	267.5	3176			67
4.	Compound no-10	272.7	270.7			14.29	68
5.	Compound no-8	277.5	267.3			13.57	68
6.	7,16-bis[2-(octoxy)benzoyl]-5,14-dihydrodibenzo[b,i][1,4,8,11]tetra azacyclotetradecine	275.2	270.2			14.41	69
7.	7,16-bis[2,2'-(pentadioxy)benzoyl]-5,14-dihydrodibenzo[b,i][1,4,8,11]tetra azacyclotetradecine	268.1	270.8			14.35	69
8.	7,16-bis[2,2'-(1,10-decanedioxy)benzoyl]-5,14-dihydrodibenzo[b,i][1,4,8,11]tetra azacyclotetradecine	273.8	270.4			14.3	69
9.	Compound no-6	275.8	269.2			14.13	69
10.	7,16-[2,2'-(1,4-bis[2-(2-ethoxy)ethoxy]benzene)benzoyl]-5,14-dihydrodibenzo[b,i][1,4,8,11]tetra azacyclotetradecine	266.2	269.5			14.19	69
11.	7,16-bis(2-hydroxybenzoyl)-5,14-dihydrodibenzo[b,i][1,4,8,11]-tetraazacyclotetradecine	274.5	270.1			14.3	70, 71
12.	Compound no. 3	273.1	268.1			14.22	72
13.	9,20-bis(2-[4-(N-pyridinium-1-yl)butoxy]benzoyl)-7,18-dihydrodinaphtho[b,i][1,4,8,11]te traazacyclotetradecine dibromide	276.6	269.7			13.51	73
14.	9,20-bis[2-(4-bromobutoxy)benzoyl]-7,18-dihydrodinaphtho[b,i][1,4,8,11]te traazacyclotetradecine	277.5	268.9			13.94	73
15.	9,20-bis[2,2'-(1,10-decanedioxy)benzoyl]-7,18-dihydrodinaphtho[b,i][1,4,8,11]te traazacyclotetradecine	274.7	268.8			13.74	73
16.	9,20-bis(3-(hydroxypropyl))-7,18-dihydrodinaphtho[b,i][1,4,8,11]te traazacyclotetradecine	275.6	268.6	3194	3176	12.72	74
17.	1,1'-(6,17-dihydrodinaphtho[2,3-b:2',3'-i][1,4,8,11]tetraazacyclotetradeci ne-8,19-diyldipropane-3,1-diyl)dipyridinium bis(bromide)	273.3	271.8	3122	3185	12.74	74
18.	7,16-dibenzoyl-6,8,15,17-tetramethyl-5,14-dihydrodibenzo(b,i)(1,4,8,11) tetraazacyclotetradecine	262	274	2800		14.2	75, 76
19.	2,3 : 9,10- dibenzo - 6,13 - dibenzoyl- 7,12 – dimthyl 5,14 - diphenyl - 1,4,8,11 - tetraazacyclotetradeca - 2,5,7,9,11,13 - hexaen (Bz,bzo,Me,Ph,[14]hexaenN4			2700		13.9	75

20.	H2TAA	264.4	269.9	3491		12.87	77
21.	6,13-Diphenyl-1,8-dihydro-2,3:9,10-dibenzo-1,4,8,11-tetra-azacyclotetradecane-4,6,11,13-tetraene	272.5	267.9			14.27	78
22.	5,14-Dihydro-7,16-dimenthyloxycarbonyl-6,17-dimethyl-8,15-diphenyl-dibenzo(b,I)(1,4,8,11)-tetraazacyclo-tetradecine	255.1	269.9			14.28	79
23.	7,16-dibenzoyl-8,17-dimethyl-6,15-diphenyl-5,14-dihydrodibenzo[b,i][1,4,8,11]tetra azacyclotetradecine	260.5	268.3			14.27	80

Table S4

No.	Name	N1N2 distance (ppm)	N2N3 distance (ppm)	ν(NH) IR (cm^{-1})	ν(NH) Raman (cm^{-1})	NMR	References
1.	bisvinylogous octaethylporphyrin	317.2	523.4			-6.61	81
2.	hemiporphycene	267.7	293.8	3140		-0.51	82
3.	hemiporphycene*	293.4	273	3040		1.14	82
4.	octaethylhemiporphycene	270.9	312.9			-2.35	83
5.	octaethylhemiporphycene*	304.5	262.7			-0.76	83
6.	2,3,8,9,14,15,20,21-octamethoxy[22]porphyrin-(2.2.2.2)	263.6	534.4			0.83	84
7.	2,3,8,9,14,15,20,21-octamethoxy-5,6,17,18-tetradehydro[22]porphyrin-(2.2.2.2)	260.8	535.5			0.86	84
8.	2,3,8,9,14,15,20,21-octaethyl(22)porphyrin(2.2.2.2)	267.4	515.4			1.34	85
9.	octaethyl acetylene-cumulene prophycene	261.8	538.7			2.28	86
10.	2,3,7,8,12,13,17,18-Octaethyl-5,10-diphenylporphyrin	260.3	791.2			2.04	87
11.	6-Aza-5,11,16-tris(4-t-butylphenyl)hemiporphycene	261.8				3.13	88
12.	6-Aza-5,11,16-tris(4-t-butylphenyl)hemiporphycene*	277.6				4.25	88
13.	(E)-octaethylisoporphycene	282.6	254.2	3357		0.1	89
14.	(E)-octaethylisoporphycene*	390.9	254.2	3398		-1.43	89
15.	DAB	285	289.7			-0.69	90
16.	Compound no. 10	280.8	281.7			-1.67	91
17.	Compound no. 9	277.9	289.5			-1.92	91
18.	10,20-di(3-chloro-2,4,6-trimethylphenyl)-5,15-diazaporphyrin	273	295.1			-2.56	91
19.	phthalocyanine	271.5	284	3275			92, 93
20.	1,4,8,11,15,18,22,25-octaethoxy-29H,31H-phthalocyanine	277.5	280.1			0.23	94
21.	1,4,8,11,15,18,22,25-octakis(cyclopentylmethyl)phthalocyanine	279.5	279.6	3301		-0.15	95
22.	1,4,8,11,15,18,22,25-octakis(cyclohexylmethyl)phthalocyanine			3297		-0.09	95
23.	2,3,6,7,11,12,17,18-octaethylcorrphycene	280.7	254.8	3283	3317		96
24.	2,3,6,7,11,12,17,18-octaethylcorrphycene	280	344.8				97
25.	2,7,11,18-tetraethyl-3,6,12,17-tetramethylcorrphycene			3274		-2.08	97
26.	2,3,7,8,17,18-hexapropyl-(1,4,5,7-tetramethyl-1,4-diazacyclohepta(2,3-l))-5,10,15,20-tetra-azaporphyrin	273.5	275.7			-2.56	98
27.	2,3,7,8,12,13,17,18-octakis(propyl)porphyrazine			3021		-2.11	99
28.	2,3,9,10,16,17,23,24-octa substituted phthalocyanine 3a			3620		-2.01	99
29.	2,3,7,8,12,13,17,18-octakis(1-naphthylmethylthio)H21, H23 porphyrazine			3326		-2.21	100

30.	1,4,14,17-tetrahydroxyhemiporphyrazine	295.2	297.2	3414			101
31.	2,3,12,13-tetrakis(trifluoromethyl)tetraphenyl porphyrin	289.4	209.9			-1.33	102, 103

* - two different molecular structures in the crystal or two different NN distances in one structure

II. Reproduction of experimental data by DFT simulations

Figures S1–S3 show correlations between calculated and experimental parameters. These plots illustrate the extent to which the selected B3LYP/6-31G(d,p) method can reproduce the experimental parameters considered in the analysis. Ideally, a linear relationship with a 45° slope (corresponding the equation $Y = X$) is expected between experimental (represented on the X-axis) and calculated (represented on the Y-axis) values. However, such ideal condition is uncommon. The accuracy of the calculated parameters is limited by the method employed and their values often contain systematic errors. For example, vibrational frequencies obtained by DFT methods usually require additional rescaling to improve their fit to the experimental values.

The crystal structure and chemical shifts are typical properties determined for newly synthesised compounds. The wide availability of these data enables their comparison with the corresponding calculated values, to estimate the accuracy of the geometric and spectroscopic parameters predicted by the simulations. The crystallographic analysis can precisely determine the relative distances between heavy atoms and the lengths of chemical bonds. In most cases, the size of the intramolecular cavity of the studied macrocycles can be defined by specifying only two distances between adjacent nitrogen atoms; due to molecular symmetry, the other two distances are almost identical. Slight differences usually result from the different local environments of the two sides of the molecule in the crystal lattice, or from differences in the configuration of the substituents. More significant differences only arise in the case of an asymmetrically substituted macrocycles .

Figure S1 shows the correlation between the two possible N...N distances, usually directed almost perpendicularly to each other. The linear correlation is described by the equation $Y = 1.02 \cdot X - 5.45$, ($R^2 = 0.95$). The data points exhibit a linear trend, except for a few points showing significant (~5 pm) shifts. This deviation is not surprising, taking into account the precision of the X-ray diffraction technique and the environment/arrangement of molecules embedded in the crystal. Moreover, the same molecule can adopt more than one crystal structure or even exhibit more than one orientation in the same structure, as observed in dibenzotetraaza[14]annulenes.[104,105] In addition, DFT simulations are performed on isolated molecules, and the functional and basis set choices affect the results.[106,107] Figure S2 shows the linear relationship between the simulated and experimental ^{1}H chemical shift values, whose correlation is described by the equation $Y = 0.91 \cdot X + 1.97$ ($R^2 = 0.97$). Only slight deviations from the corresponding straight line are visible. The chemical shifts of the protons participating in a hydrogen bond are not strongly affected by the molecular environment when the protons are located in the cavity. The discrepancy is even smaller when each macrocycle family is considered separately. In such a case, the data points of each family show an almost linear trend, but the slopes of the corresponding fitted lines are slightly different. Similarly, a slight scattering

of points around the fitting line is observed in Figure S3, which compares the simulated and experimental values of the NH stretching frequency. The points marked in Figure S3 with letters A, B, and C were excluded from the fitting (we expect their experimental values are the result of a wrong assessment), and the intercept was fixed at 0. The resulting correlation is described by the equation $Y = 0.93 \cdot X$ ($R^2 = 0.9997$).

Because the NH stretching bands of porphyrin-like molecules in the vibrational (IR and Raman) spectra are very weak and often appear close to the CH bands, their frequencies are rarely reported; therefore, only a small number of NH stretching frequency data points are considered in the present study. A few points marked with the capital letters A, B, and C strongly deviate from the fitting line, whereas the NH stretching frequencies for all other porphyrin and dibenzotetraaza[14]annulene derivatives are located close to the line. The experimental values of the three outlier points (A, B, and C) are close to 3400 cm^{-1}. The broad band corresponding to water molecules bonded in the KBr salt or to ice deposited on the cooled detector window also appears in this spectral region (~3400 cm^{-1}), and may be incorrectly assigned to the NH stretching mode. These points were not considered in the fitting calculation.

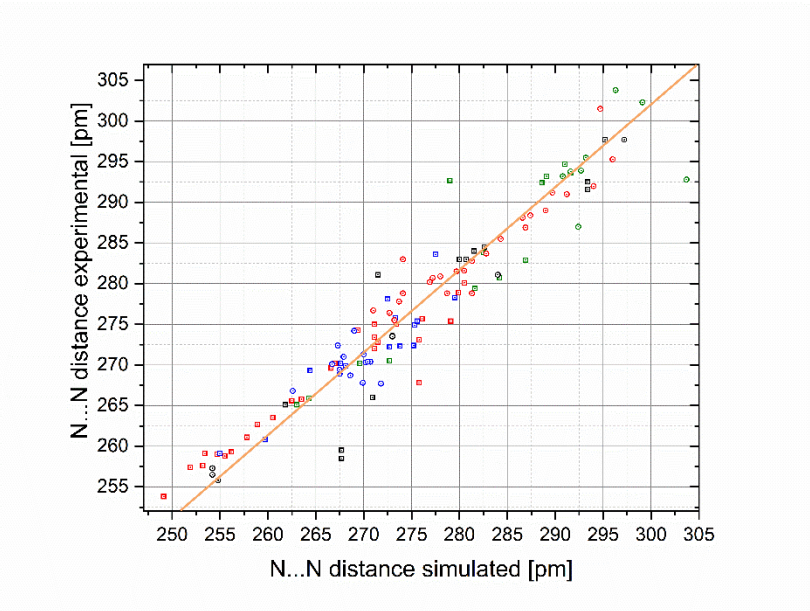

Figure S1. Relationship between the calculated and experimental N…N distances in porphyrins (green), porphycenes (red), dibenzotetraaza[14]annulenes (blue), and other macrocycles (black). Squares represents N…N distances along hydrogen bond and circles are N…N distances along the other N…N direction. The line is the linear fitting to the datapoints.

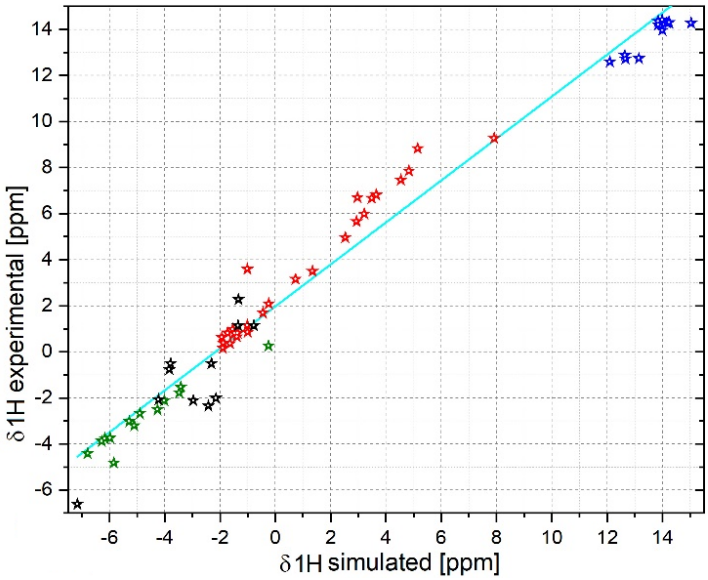

Figure S2. Relationship between the calculated and experimental ^{1}H chemical shifts in porphyrins (green), porphycenes (red), dibenzotetraaza[14]annulenes (blue), and other macrocycles (black). The line is the linear fitting to the datapoints.

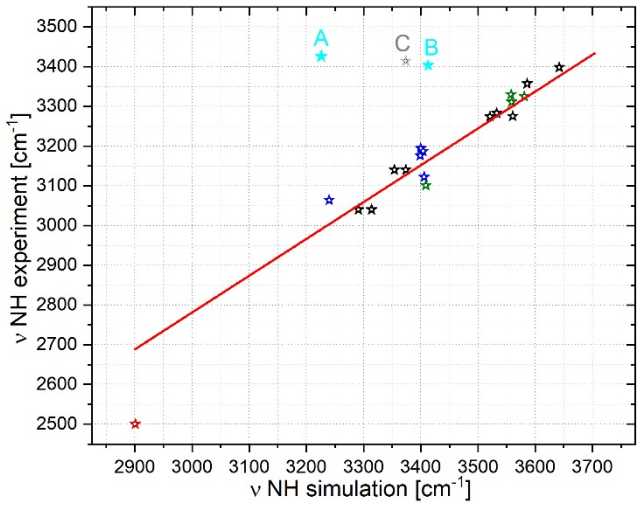

Figure S3. Relationship between the calculated and experimental NH stretching mode frequencies in porphyrins (green), porphycenes (red), dibenzotetraaza[14]annulenes (dark and light blue), and other macrocycles (black and grey). Points marked with letters A, B represent porphyrin derivatives, and point C denotes dibenzotetraaza[14]annulene derivative. Red line represents linear fit with the intercept fixed at 0.

III. Fitting plots of experimental and simulation data

The results of fitting with linear or second-order functions of the experimental and simulated (fully optimised molecular structures) are presented. On each figure, open circles represent data points extracted from the result of simulations for fully optimised molecular geometries. Stars represent experimental data points taken from the literature. All fitting curves are held red but different colours of data points are used to represent different macrocycles families: red for porphycenes, green for porphyrins, and blue for dibezotetraaza[14]annulenes. All fittings were performed with the algorithm inbuild in Origin 2020b software.

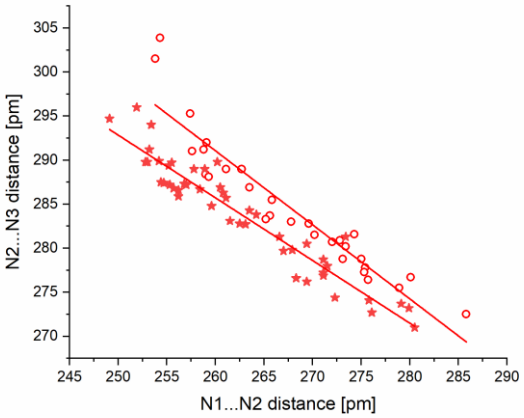

Figure S4. Relationships between two N…N distances (N1…N2: distance along a hydrogen bond, N2…N3: distance between nitrogen atoms not forming a hydrogen bond) in porphycenes. Stars represent experimental data, and circles denote calculated values for fully optimised molecular structures. Lines represent fittings of datapoints of:

- simulation: $Y = -(0.84 \pm 0.056) \cdot X + (510 \pm 15)$, $R^2 = 0.885$
- experiment: $Y = -(0.71 \pm 0.031) \cdot X + (471 \pm 8)$, $R^2 = 0.911$

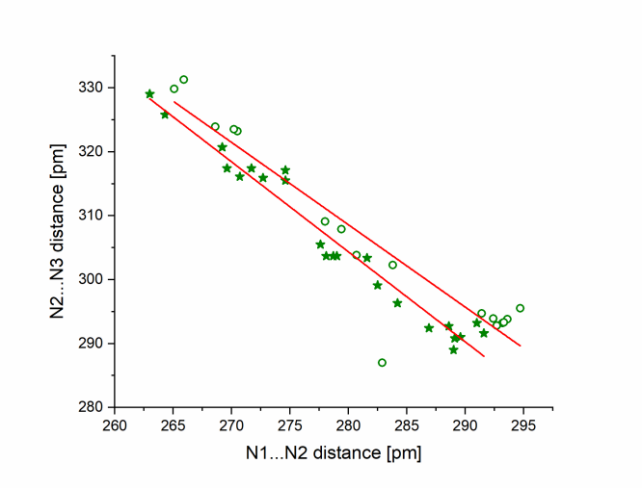

Figure S5. Relationships between two N…N distances (N1…N2: distance along a hydrogen bond, N2…N3: distance between nitrogen atoms not forming a hydrogen bond) in porphyrins. Stars represent experimental data, and circles denote calculated values for fully optimised molecular structures. Lines represent fittings of datapoints of:

- simulation: $Y = -(1.29 \pm 0.12) \cdot X + (669 \pm 35)$, $R^2 = 0.871$
- experiment: $Y = -(1.41 \pm 0.06) \cdot X + (698 \pm 17)$, $R^2 = 0.96$

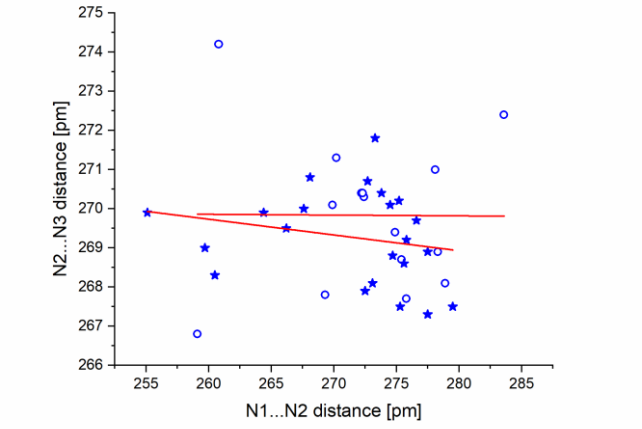

Figure S6. Relationships between two N…N distances (N1…N2: distance along a hydrogen bond, N2…N3: distance between nitrogen atoms not forming a hydrogen bond) in dibenzotetraaza[14]annulenes. Stars represent experimental data, and circles denote calculated values for fully optimised molecular structures. Lines represent fittings of data points of:

- simulation: $Y = -(0.002 \pm 0.083) \cdot X + (270 \pm 23)$, $R^2 = 0.077$
- experiment: $Y = -(0.040 \pm 0.040) \cdot X + (280 \pm 11)$, $R^2 = 0.000$

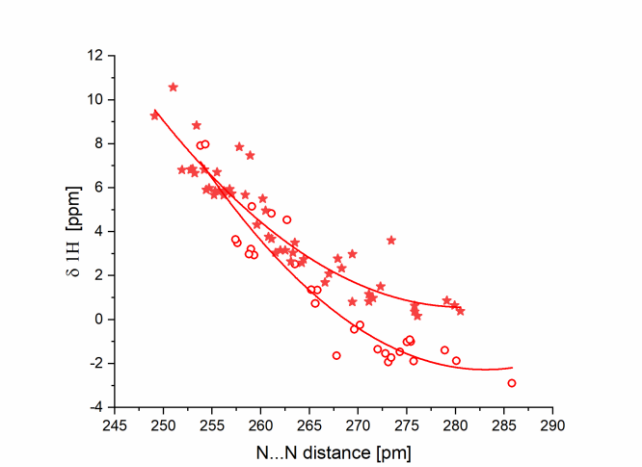

Figure S7. Relationships between N…N distance along hydrogen bond and ^{1}H chemical shift in porphycenes. Stars represent experimental data, and circles denote calculated values for fully optimised molecular structures. Lines represent fittings of datapoints of:

- simulation: $Y = (0.011 \pm 0.002) \cdot X^2 - (6.25 \pm 1.39) \cdot X + (882 \pm 186)$, $R^2 = 0.893$
- experiment: $Y = (0.0089 \pm 0.0018) \cdot X^2 - (4.99 \pm 0.98) \cdot X + (702 \pm 129)$, $R^2 = 0.876$

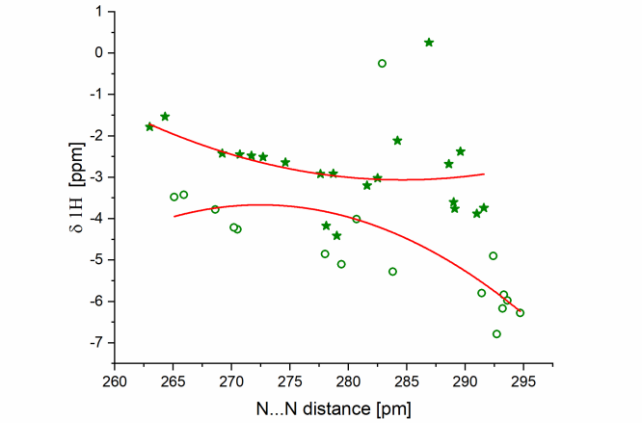

Figure S8. Relationships between N…N distance along hydrogen bond and ^{1}H chemical shift in porphyrins. Stars represent experimental data, and circles denote calculated values for fully optimised molecular structures. Lines represent fittings of datapoints of:

- simulation: $Y = -(0.0052 \pm 0.0039) \cdot X^2 - (2.83 \pm 2.19) \cdot X + (390 \pm 307)$, $R^2 = 0.343$
- experiment: $Y = (0.0029 \pm 0.0032) \cdot X^2 - (1.63 \pm 1.76) \cdot X + (229 \pm 245)$, $R^2 = 0.038$

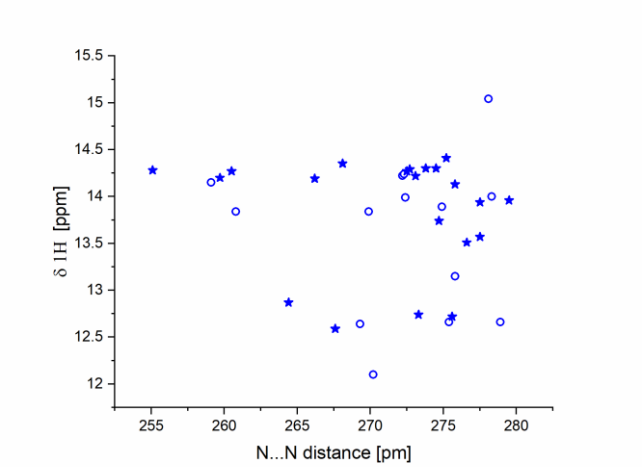

Figure S9. Relationships between N…N distance along hydrogen bond and ^{1}H chemical shift in dibenzotetraaza[14]annulenes. Stars represent experimental data, and circles denote calculated values for fully optimised molecular structures. Due to large scattering of datapoints they were not fitted.

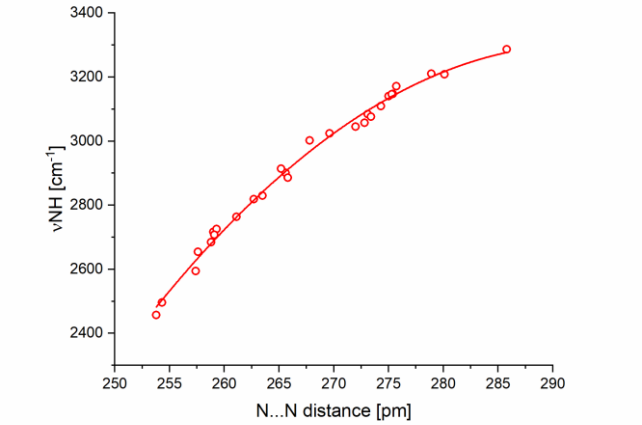

Figure S10. Relationships between N…N distance along hydrogen bond and NH stretching frequency in porphycenes. Circles denote calculated values for fully optimised molecular structures. Line represents fitting of datapoints: $Y = -(0.55 \pm 0.05) \cdot X^2 + (320 \pm 28) \cdot X - (43488 \pm 3761)$, $R^2 = 0.992$

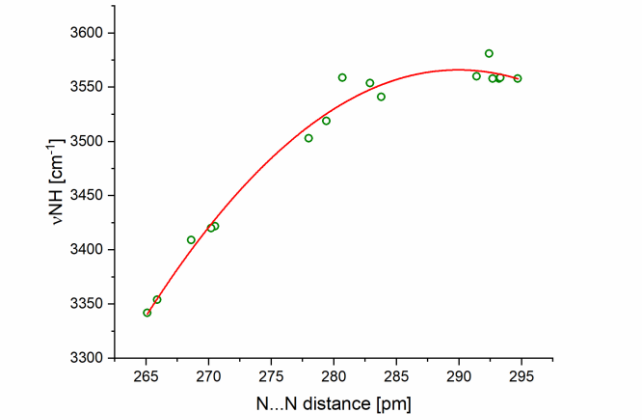

Figure S11. Relationships between N…N distance along hydrogen bond and NH stretching frequency in porphyrins. Circles denote calculated values for fully optimised molecular structures. Line represents fitting of datapoints: $Y = -(0.36 \pm 0.03) \cdot X^2 + (211 \pm 19) \cdot X - (27096 \pm 2602)$, $R^2 = 0.983$

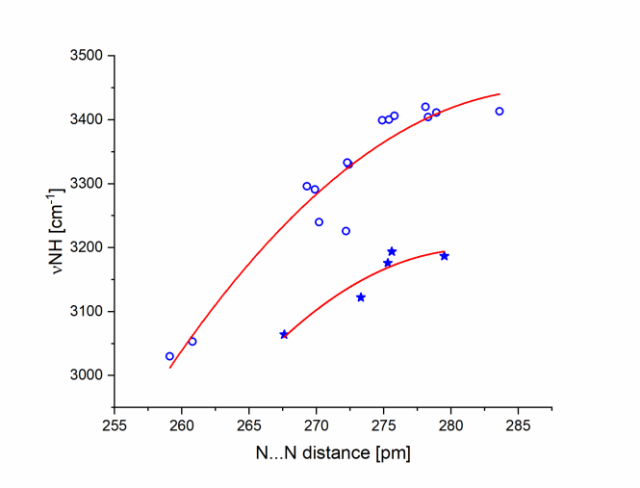

Figure S12. Relationships between N…N distance along hydrogen bond and NH stretching frequency in dibenzotetraaza[14]annulenes. Stars represent experimental data, and circles denote calculated values for fully optimised molecular structures. Lines represent fittings of datapoints:

- simulation: $Y = -(0.55 \pm 0.19) \cdot X^2 + (315 \pm 103) \cdot X - (41788 \pm 13967)$, $R^2 = 0.911$
- experiment: $Y = -(0.68 \pm 0.71) \cdot X^2 + (384 \pm 391) \cdot X - (50955 \pm 53427)$, $R^2 = 0.783$

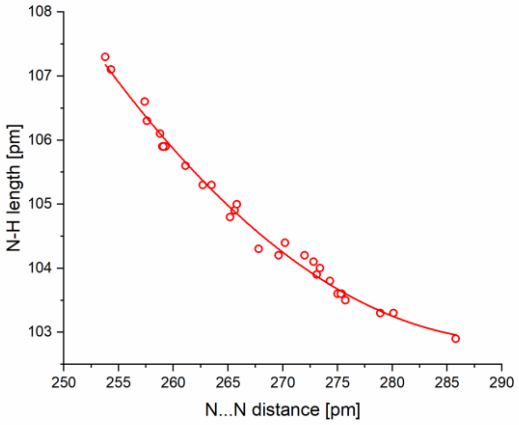

Figure S13. Relationships between N…N distance along hydrogen bond and NH bond length in porphycenes. Circles denote calculated values for fully optimised molecular structures. Line represents fitting of datapoints: $Y = (0.0031 \pm 0.0003) \cdot X^2 - (1.80 \pm 0.17) \cdot X + (365 \pm 23)$, $R^2 = 0.989$

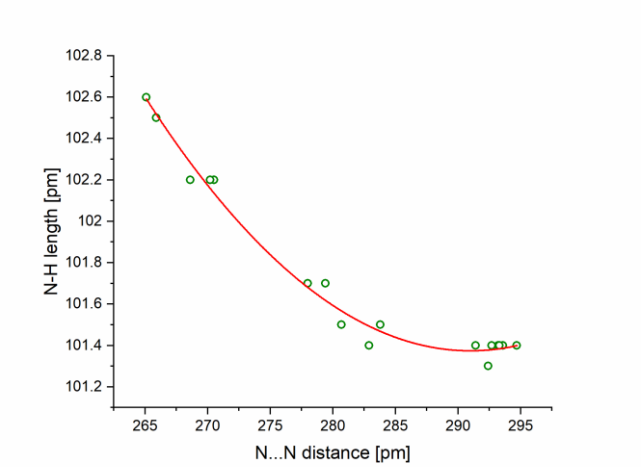

Figure S14. Relationships between N…N distance along hydrogen bond and NH bond length in porphyrins. Circles denote calculated values for fully optimised molecular structures. Line represents fitting of datapoints:
$Y = (0.0018 \pm 0.0002) \cdot X^2 - (1.06 \pm 0.09) \cdot X + (255 \pm 13)$, $R^2 = 0.984$

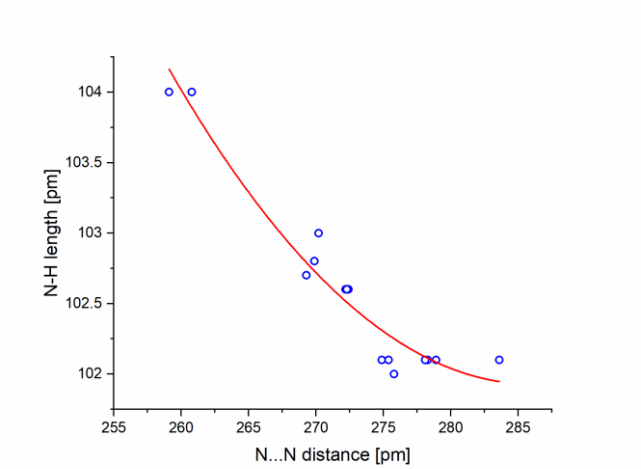

Figure S15. Relationships between N…N distance along hydrogen bond and NH bond length in dibenzotetraaza[14]annulenes. Circles denote calculated values for fully optimised molecular structures. Line represents fitting of datapoints:
$Y = (0.0031 \pm 0.0008) \cdot X^2 - (1.77 \pm 0.45) \cdot X + (354 \pm 61)$, $R^2 = 0.936$

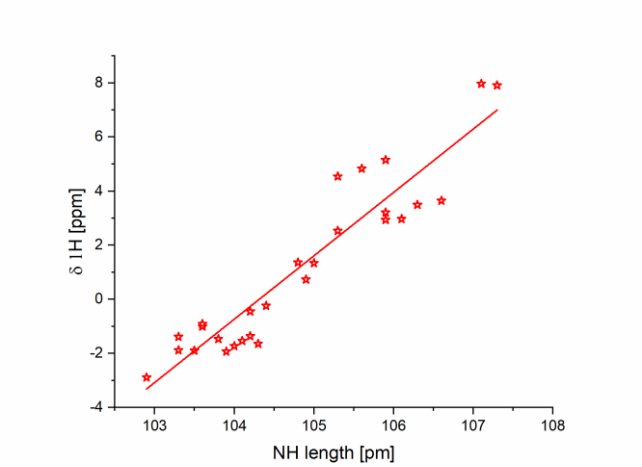

Figure S16. Relationships between NH bond length and ^{1}H chemical shift in porphycenes. Stars represent calculated values for fully optimised molecular structures. Line represents fitting of datapoints:
$Y = (2.34 \pm 0.16) \cdot X - (244 \pm 17)$, $R^2 = 0.881$

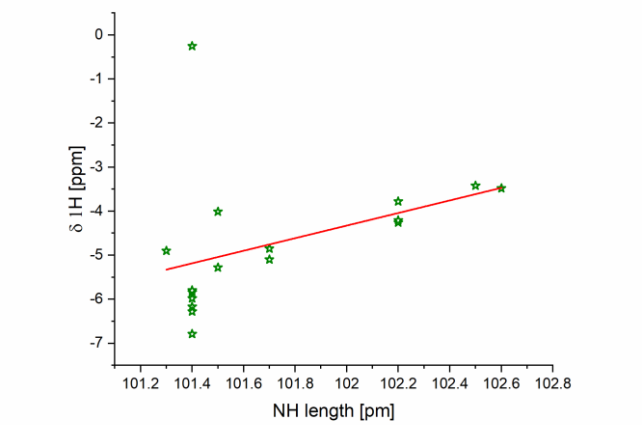

Figure S17. Relationships between NH bond length and ^{1}H chemical shift in porphyrins. Stars represent calculated values for fully optimised molecular structures. Line represents fitting of datapoints:
$Y = (1.43 \pm 0.84) \cdot X - (150 \pm 85)$, $R^2 = 0.107$

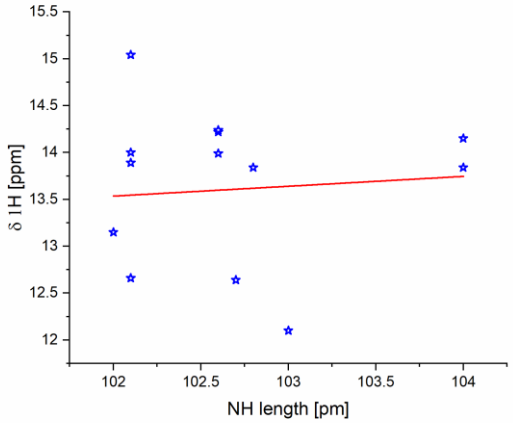

Figure S18. Relationships between NH bond length and ^{1}H chemical shift in dibenzotetraaza[14]annulenes. Stars represent calculated values for fully optimised molecular structures. Line represents fitting of datapoints:
$Y = (0.105 \pm 0.357) \cdot X - (2.809 \pm 36.6)$, $R^2 = 0.075$

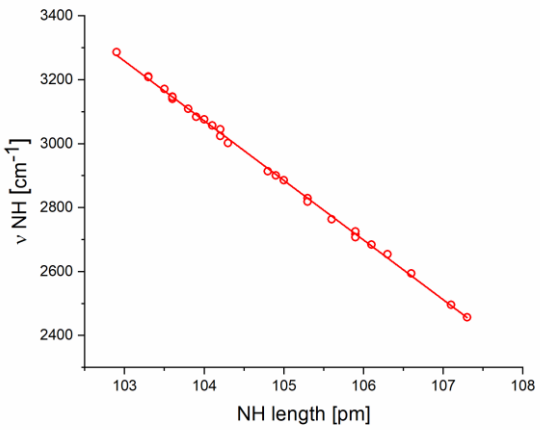

Figure S19. Relationships between NH bond length and NH stretching mode frequency in porphycenes. Circles denote calculated values for fully optimised molecular structures. Line represents fitting of datapoints:
$Y = (22465 \pm 116) \cdot X - (186 \pm 1)$, $R^2 = 0.999$

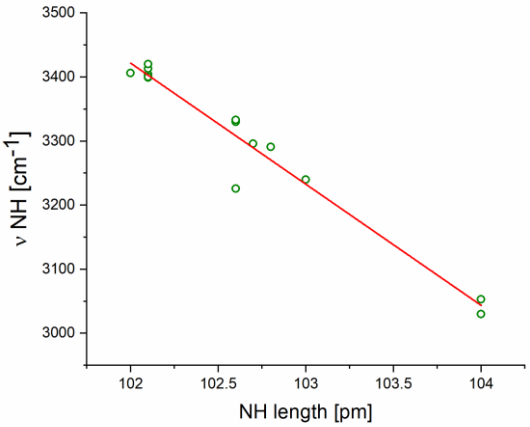

Figure S20. Relationships between NH bond length and NH stretching mode frequency in porphyrins. Circles denote calculated values for fully optimised molecular structures. Line represents fitting of datapoints:
$Y = (22701 \pm 1195) \cdot X - (189 \pm 12)$, $R^2 = 0.95$

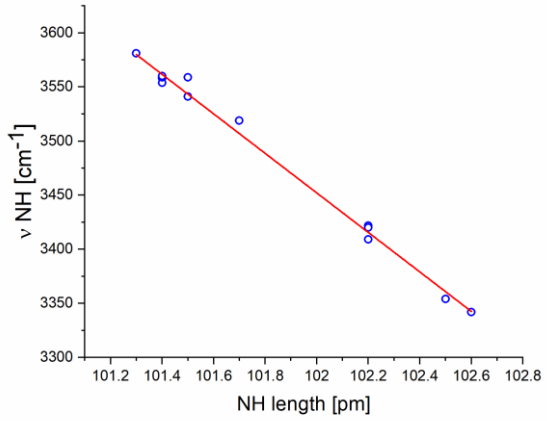

Figure S21. Relationships between NH bond length and NH stretching mode frequency in dibenzotetraaza[14]annulenes. Circles denote calculated values for fully optimised molecular structures. Line represents fitting of datapoints:
$Y = (22077 \pm 420) \cdot X - (183 \pm 4)$, $R^2 = 0.993$

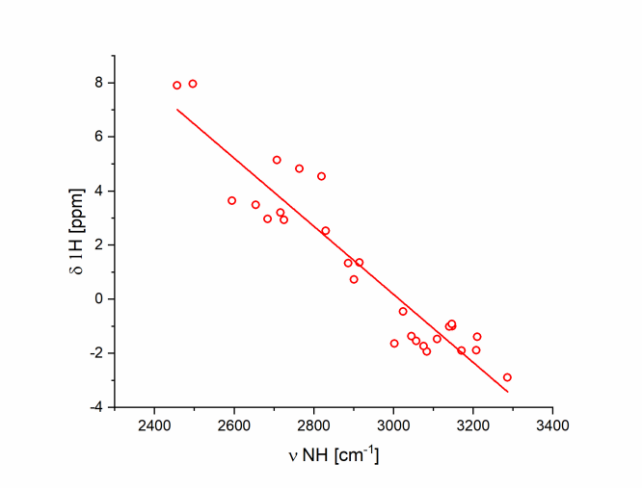

Figure S22. Relationships between NH stretching mode frequency and ^{1}H chemical shift in porphycenes. Circles denote calculated values for fully optimised molecular structures. Line represents fitting of datapoints: $Y = -(0.0126 \pm 0.001) \cdot X + (37.9 \pm 2.5)$, $R^2 = 0.886$

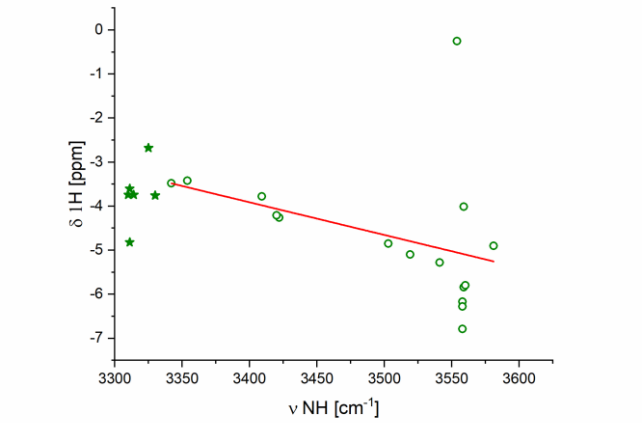

Figure S23. Relationships between NH stretching mode frequency and ^{1}H chemical shift in porphyrins. Stars represent experimental data and circles denote calculated values for fully optimised molecular structures. Line represents fitting of datapoints:

- simulation: $Y = -(0.0074 \pm 0.0047) \cdot X + (21.2 \pm 16.6)$, $R^2 = 0.087$
- experiment: Not fitted.

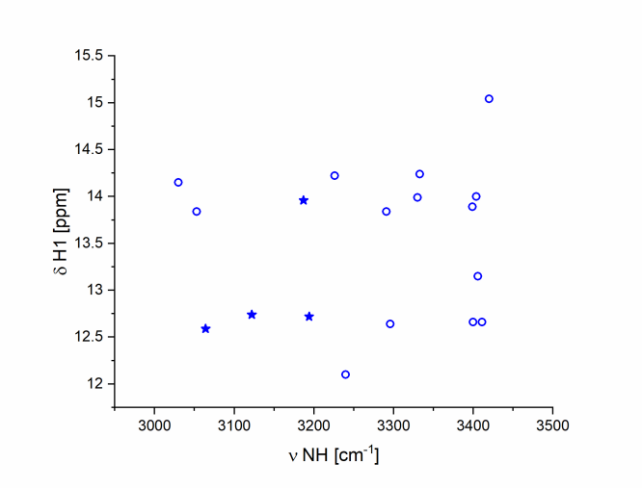

Figure S24. Relationships between NH stretching mode frequency and ^{1}H chemical shift in dibenzotetraaza[14]annulenes. Stars represent experimental data and circles denote calculated values for fully optimised molecular structures. Not fitted.

IV. References

1. E. Vogel, M. Köcher, H. Schmickler and J. Lex, *Angewandte Chemie*, 1986, 25, 257-259.
2. S. Gawinkowski, Ł. Walewski, A. Vdovin, A. Slenczka, S. Rols, M. R. Johnson, B. Lesyng and J. Waluk, *Physical Chemistry Chemical Physics*, 2012, 14, 5489-5503.
3. J. N. Ladenthin, T. Frederiksen, M. Persson, J. C. Sharp, S. Gawinkowski, J. Waluk and T. Kumagai, *Nature Chemistry*, 2016, 8, 935-940.
4. P. Fita, N. Urbańska, C. Radzewicz and J. Waluk, *Chemistry – A European Journal*, 2009, 15, 4851-4856.
5. T. Ono, D. Koga and Y. Hisaeda, *Chemical Communications*, 2017, 46, 260-262.
6. E. Vogel, M. Köcher, J. Lex and O. Ermer, *Israel Journal of Chemistry,* 1989, 29, 257-266.
7. T. Ono, N. Xu, D. Koga, T. Ideo, M. Sugimoto and Y. Hisaeda, *RSC Advances*, 2018, 8, 39269-39273.
8. N. N. Pati, S. Sahoo, S. S. Sahoo, D. Banerjee, S. V. Rao and P. K. Panda, *New Journal of Chemistry*, 2020, 44, 9616-9620.
9. D. Kuzuhara, H. Yamada, K. Yano, T. Okujima, S. Mori and H. Uno, *Chemistry – A European Journal*, 2011, 17, 3376-3383.
10. E. Vogel, P. Koch, X.-L. Hou, J. Lex, M. Lausmann, M. Kisters, M. A. Aukauloo, P. Richard and R. Guilard, *Angewandte Chemie*, 1993, 32, 1600-1604.
11. T. Ono, D. Koga, K. Yoza and Y. Hisaeda, *Chemical Communications*, 2017, 53, 12258-12261.
12. K. Oohora, A. Ogawa, T. Fukuda, A. Onoda, J.-y. Hasegawa and T. Hayashi, *Angewandte Chemie*, 2015, 54, 6227-6230.
13. E. Vogel, M. Balci, K. Pramod, P. Koch, J. Lex and O. Ermer, *Angewandte Chemie,* 1987, 26, 928-931.
14. Y. Nosenko, J. Jasny, M. Pietraszkiewicz, A. Mordzinski, *Chemical Physics Letters,* 399 (2004) 331–336.
15. S. Nonell, N. Bou, J. Borrell, J. Teixidó, A. Villanueva, A. Juarranz and M. Cañete, *Tetrahedron Letters*, 1995, 36, 3405-3408.
16. D. Kuzuhara, H. Nakaoka, T. Okabe, N. Aratani and H. J. H. Yamada, *Heterocycles*, 2015, 90, 1214.
17. T. Sarma, P. K. Panda, P. T. Anusha and S. V. Rao, *Organic Letters*, 2011, 13, 188-191.
18. M. Pietrzak, M. F. Shibl, M. Bröring, O. Kühn and H.-H. Limbach, *Journal of the American Chemical Society*, 2007, 129, 296-304.
19. A. Rana, B. S. Kumar and P. K. Panda, *Organic Letters*, 2020, 22, 7175-7180.
20. A. Rana and P. K. Panda, *Organic Letters*, 2014, 16, 78-81.
21. T. Hayashi, Y. Nakashima, K. Ito, T. Ikegami, I. Aritome, A. Suzuki and Y. Hisaeda, *Organic Letters*, 2003, 5, 2845-2848.
22. H. Shimakoshi, T. Baba, Y. Iseki, I. Aritome, A. Endo, C. Adachi and Y. Hisaeda, *Chemical Communications*, 2008, 25, 2882-2884.
23. S. Will, A. Rahbar, H. Schmickler, J. Lex and E. Vogel, *Angewandte Chemie,* 1990, 29, 1390-1393.
24. N. N. Pati, B. S. Kumar and P. K. Panda, *Organic Letters*, 2017, 19, 134-137.
25. D. Kuzuhara, J. Mack, H. Yamada, T. Okujima, N. Ono and N. Kobayashi, *Chemistry – A European Journal*, 2009, 15, 10060-10069.
26. D. Kuzuhara, H. Yamada, S. Moric, T. Okujimad and H. Uno, *Journal of Porphyrins and Phthalocyanines*, 2011, 15, 930–942.
27. T. Okawara, M. Abe and Y. Hisaeda, *Tetrahedron Letters*, 2014, 55, 6193-6197.
28. T. Okabe, D. Kuzuhara, N. Aratani and H. Yamada, *Journal of Porphyrins and Phthalocyanines,* 2014, 18, 849-855.
29. T. Ono, H. Shinjo, D. Koga and Y. Hisaeda, *European Journal of Organic Chemistry*, 2019, 7578-7583.
30. A. Rana, S. Lee, D. Kim and P. K. Panda, *Chemical Communications*, 2015, 51, 7705-7708.
31. A. Rana and P. K. Panda, *Chemical Communications*, 2015, 51, 12239-12242.
32. N. Xu, T. Ono and Y. Hisaeda, *Chemistry — A European Journal*, 2019, 25, 11680-11687.
33. D. Kuzuhara, H. Nakaoka, K. Matsuo, N. Aratani and H. Yamada, *Journal of Porphyrins and Phthalocyanines,* 2019, 23, 898-907.

34. J. G. Radziszewski, M. Nepras, V. Balaji, J. Waluk, E. Vogel and J. Michl, *The Journal of Physical Chemistry*, 1995, 99, 14254-14260.
35. E. D. Becker and R. B. Bradley, *The Journal of Chemical Physics*, 1959, 31, 1413-1414.
36. K. N. Solov'ev, V. A. Mashenkov, A. T. Gradyushko, A. E. Turkova and V. P. Lezina, *Journal of Applied Spectroscopy*, 1970, 13, 1106-1111.
37. P. M. Kozlowski, A. A. Jarzęcki, P. Pulay, X.-Y. Li and M. Z. Zgierski, *The Journal of Physical Chemistry*, 1996, 100, 13985-13992.
38. I. Saltsman, I. Goldberg, Y. Balasz and Z. Gross, *Tetrahedron Letters*, 2007, 48, 239-244.
39. L. E. Webb and E. B. Fleischer, *The Journal of Chemical Physics*, 1965, 43, 3100-3111.
40. M. O. Senge and I. Bischoff, *European Journal of Organic Chemistry*, 2001, 2001, 1735-1751.
41. S. Gawinkowski, G. Orzanowska, K. Izdebska, M. O. Senge and J. Waluk, *Chemistry – A European Journal,* 2011, 17, 10039-10049.
42. M. Pietrzak, M. F. Shibl, M. Bröring, O. Kühn and H.-H. Limbach, *Journal of the American Chemical Society*, 2007, 129, 296-304.
43. S. F. Mason, *Journal of the Chemical Society*, 1958, 0, 976-982.
44. M. O. Senge, C. J. Medforth, T. P. Forsyth, D. A. Lee, M. M. Olmstead, W. Jentzen, R. K. Pandey, J. A. Shelnutt and K. M. Smith, *Inorganic Chemistry*, 1997, 36, 1149-1163.
45. C. J. Medforth, M. O. Senge, T. P. Forsyth, J. D. Hobbs, J. A. Shelnutt and K. M. Smith, *Inorganic Chemistry*, 1994, 33, 3865-3872.
46. E. J. R. Sudhöulter, M. van Dijk, C. J. Teunis, G. M. Sanders, S. Harkema, G. M. H. van de Velde, P. G. Schouten and J. M. Warman, *Journal of Materials Chemistry*, 1996, 6, 357-363.
47. A. D. Bond, N. Feeder, J. E. Redman, S. J. Teat and J. K. M. Sanders, *Crystal Growth & Design*, 2002, 2, 27-39.
48. J. S. Manka and D. S. Lawrence, *Tetrahedron Letters*, 1989, 30, 6989-6992.
49. C. J. Kingsbury, K. J. Flanagan, H.-G. Eckhardt, M. Kielmann and M. O. Senge, *Molecules*, 2020, 25, 3195.
50. L. Zhou, Z.-X. Xu, Y. Zhou, Y. Feng, X.-G. Zhou, H.-F. Xiang and V. A. L. Roy, *Chemical Communications*, 2012, 48, 5139-5141.
51. M. O. Senge, W. W. Kalisch and I. Bischoff, *Chemistry – A European Journal*, 2000, 6, 2721-2738.
52. Q. Liu, J. Zhang, M. Tang, Y. Yang, J. Zhang and Z. Zhou, *Organic & Biomolecular Chemistry*, 2018, 16, 7725-7736.
53. T. Chandra, B. J. Kraft, J. C. Huffman and J. M. Zaleski, *Inorganic Chemistry*, 2003, 42, 5158-5172.
54. P. J. Commins, J. P. Hill, Y. Matsushita, W. A. Webre, J. Labuta, K. Ariga and F. D'Souza, *Journal of Porphyrins and Phthalocyanines,* 2016, 20, 213-222.
55. S. Sugawara, T. Kakui and Y. Yamamoto, *Journal of Porphyrins and Phthalocyanines,* 2014, 18, 975-981.
56. P. K. Panda and V. Krishnan, *Journal of Chemical Sciences*, 2005, 117, 73-84.
57. A. Merz, R. Schropp and J. Lex, *Angewandte Chemie*, 1993, 32, 291-293.
58. Z. Shen, H. Uno, Y. Shimizu and N. Ono, *Organic & Biomolecular Chemistry*, 2004, 2, 3442-3447.
59. K. Maruyama, T. Nagata and A. Osuka, *Journal of Physical Organic Chemistry*, 1988, 1, 63-73.
60. J. L. Sessler, E. A. Brucker, V. Lynch, M. Choe, S. Sorey and E. Vogel, *Chemistry — A European Journal*, 1996, 2, 1527-1532.
61. A. Rana and P. K. Panda, *Tetrahedron Letters*, 2011, 52, 2697-2701.
62. A. Merz, R. Schropp and J. Lex, *Angewandte Chemie*, 1993, 32, 291-293.
63. N. Azuma, H. Tani, T. Ozawa, H. Niida, K. Tajima and K. Sakata, *Journal of the Chemical Society, Perkin Transactions 2*, 1995, 343-348.
64. J. O. Alben, S. S. Choi, A. D. Adler and W. S. Caughey, *Annals of the New York Academy of Sciences*, 1973, 206, 278-295.
65. V. L. Goedken, J. J. Pluth, S.-M. Peng and B. Bursten, *Journal of the American Chemical Society*, 1976, 98, 8014-8021.
66. H. Schumann, B. Neumann and H.-G. Stammler, *Zeitschrift für Naturforschung B,* 1996, 51, 1255-1266.
67. P. J. Lukes, J. A. Crayston, D. J. Ando, M. E. Harman and M. B. Hursthouse, *Journal of the Chemical Society, Perkin Transactions 2*, 1991, 1845-1849.

68. D. Pawlica, M. Radić-Stojković, Ł. Dudek, I. Piantanida, L. Sieroń and J. Eilmes, *Tetrahedron*, 2009, 65, 3980-3989.
69. J. Grolik, K. Zwoliński, L. Sieroń and J. Eilmes, *Tetrahedron*, 2011, 67, 2623-2632.
70. J. Grolik, L. Sieroń and J. Eilmes, *Tetrahedron Letters*, 2006, 47, 8209-8213.
71. I. Sigg, G. Haas and T. Winkler, 1982, 65, 275-279.
72. Ł. Dudek, J. Grolik, A. Kaźmierska, E. Szneler, A. Eilmes, K. Stadnicka and J. Eilmes, *Tetrahedron Letters*, 2011, 52, 3597-3601.
73. A. Kaźmierska, M. Gryl, K. Stadnicka and J. Eilmes, *Supramolecular Chemistry*, 2013, 25, 276-285.
74. A. Kaźmierska, M. Gryl, K. Stadnicka, L. Sieroń, A. Eilmes, J. Nowak, M. Matković, M. Radić-Stojković, I. Piantanida and J. Eilmes, *Tetrahedron*, 2015, 71, 4163-4173.
75. J. Eilmes, *Polyhedron*, 1985, 4, 943-946.
76. J. Śliwiński, J. Eilmes, B. J. Oleksyn and K. Stadnicka, *Journal of Molecular Structure*, 2004, 694, 1-19.
77. J. Eilmes, M. Basato and G. Valle, *Inorganica Chimica Acta*, 1999, 290, 14-20.
78. J. Jubb, L. F. Larkworthy, D. C. Povey and G. W. Smith, *Polyhedron*, 1993, 12, 1179-1185.
79. J. Eilmes, O. Michalski and K. Woźniak, *Inorganica Chimica Acta*, 2001, 317, 103-113.
80. Y. Shen, H. Xue, Y.-Q. Wei, M. Shen, R.-C. Xu, X. Wang, X. Shen and D.-R. Zhu, *Journal of Inclusion Phenomena and Macrocyclic Chemistry*, 2016, 86, 191-199.
81. H. König, C. Eickmeier, M. Möller, U. Rodewald and B. Franck, *Angewandte Chemie*, 1990, 29, 1393-1395.
82. J. Ostapko, K. Nawara, M. Kijak, J. Buczyńska, B. Leśniewska, M. Pietrzak, G. Orzanowska and J. Waluk, *Chemistry – A European Journal,* 2016, 22, 17311-17320.
83. E. Vogel, M. Bröring, S. J. Weghorn, P. Scholz, R. Deponte, J. Lex, H. Schmickler, K. Schaffner, S. E. Braslavsky, M. Müller, S. Pörting, J. L. Sessler and C. J. Fowler, *Angewandte Chemie*, 1997, 36, 1651-1654.
84. A. Rana, S. Lee, D. Kim and P. K. Panda, *Chemistry – A European Journal*, 2015, 21, 12129-12135.
85. E. Vogel, N. Jux, E. Rodriguez-Val, J. Lex and H. Schmickler, *ChemInform,* 1991, 22.
86. N. Jux, P. Koch, H. Schmickler, J. Lex and E. Vogel, *Angewandte Chemie*, 1990, 29, 1385-1387.
87. D. O. Martire, N. Jux, P. F. Aramendia, R. Martin Negri, J. Lex, S. E. Braslavsky, K. Schaffner and E. Vogel, *Journal of the American Chemical Society*, 1992, 114, 9969-9978.
88. F. Mandoj, M. Stefanelli, S. Nardis, M. Mastroianni, F. R. Fronczek, K. M. Smith and R. Paolesse, *Chemical Communications*, 2009, 12, 1580-1582.
89. E. Vogel, P. Scholz, R. Demuth, C. Erben, M. Bröring, H. Schmickler, J. Lex, G. Hohlneicher, D. Bremm and Y.-D. Wu, *Angewandte Chemie*, 1999, 38, 2919-2923.
90. J.-F. Longevial, A. Yamaji, D. Aggad, G. Kim, W. X. Chia, T. Nishimura, Y. Miyake, S. Clément, J. Oh, M. Daurat, C. Nguyen, D. Kim, M. Gary-Bobo, S. Richeter and H. Shinokubo, *Chemical Communications*, 2018, 54, 13829-13832.
91. J.-F. Longevial, K. Miyagawa and H. Shinokubo, *Dalton Transactions*, 2020, 49, 14786-14789.
92. J. Kügel, L. Klein, M. Leisegang and M. Bode, *The Journal of Physical Chemistry C*, 2017, 121, 28204-28210.
93. H. Jiang, P. Hu, J. Ye, R. Ganguly, Y. Li, Y. Long, D. Fichou, W. Hu and C. Kloc, *Angewandte Chemie,* 2018, 57, 10112-10117.
94. M. Peterson, C. Hunt, Z. Wang, S. E. Heinrich, G. Wu and G. Ménard, *Dalton Transactions*, 2020, 49, 16268-16277.
95. A. N. Cammidge, C.-H. Tseng, I. Chambrier, D. L. Hughes, M. J. Cook, *Tetrahedron Letters*, 2000, 50, 5254-5256.
96. A. Gorski, B. Leśniewska, G. Orzanowska and J. Waluk, *Journal of Porphyrins and Phthalocyanines,* 2016, 20, 367-377.
97. J. L. Sessler, E. A. Brucker, S. J. Weghorn, M. Kisterms, M. Schaefer, J. Lex and E. Vogel, *ChemInform*, 1995, 26.

98. S. M. Baum, A. A. Trabanco, A. G. Montalban, A. S. Micallef, C. Zhong, H. G. Meunier, K. Suhling, D. Phillips, A. J. P. White, D. J. Williams, A. G. M. Barrett and B. M. Hoffman, *The Journal of Organic Chemistry*, 2003, 68, 1665-1670.
99. D. A. Isabirye, F. M. Mtunzi and T. O. Aiyelabola, *Dyes and Pigments*, 2014, 109, 214-222.
100. E. Gonca, Y. Köseoğlu, B. Aktaş and A. Gül, *Polyhedron*, 2004, 23, 1845-1849.
101. M. Ruf, W. S. Durfee and C. G. Pierpont, *Chemical Communications*, 2004, 8, 1022-1023.
102. C. Liu and Q.-Y. Chen, *European Journal of Organic Chemistry*, 2005, 2005, 3680-3686.
103. K. E. Thomas, J. Conradie, C. M. Beavers and A. Ghosh, *Organic & Biomolecular Chemistry*, 2020, 18, 2861-2865.
104. E. Sister, V. Gottfried, M. Kapon, M. Kaftory, Z. Dori and H. B. Gray, *Inorganic Chemistry*, 1988, 27, 600-604.
105. N. Azuma, H. Tani, T. Ozawa, H. Niida, K. Tajima and K. Sakata, *Journal of Chemical Society, Perkin Transactions 2*, 1995, 343-348.
106. J. A. Plumley and J. J. Dannenberg, *Journal of Computational Chemistry*, 2011, 32, 1519-1527.
107. A. Gorski, S. Gawinkowski, J. Herbich, O. Krauss, B. Brutschy, R. P. Thummel and J. Waluk, *Journal of Physical Chemistry A*, 2012, 116, 11973-11986.